FLUENCE MAP OPTIMIZATION IN INTENSITY MODULATED RADIATION THERAPY FOR FUZZY TARGET DOSE

A. FAKHARZADEH JAHROMI, O. BOZORG, H. MALEKI AND M. A. MOSLEH-SHIRAZI

Abstract. Although many methods exist for intensity modulated radiotherapy (IMRT) fluence map optimization for crisp data, based on clinical practice, some of the involved parameters are fuzzy. In this paper, the best fluence maps for an IMRT procedure were identifed as a solution of an optimization problem with a quadratic objective function, where the prescribed target dose vector was fuzzy. First, a defuzzying procedure was introduced to change the fuzzy model of the problem into an equivalent non-fuzzy one. Since the solution set was nonconvex, the optimal solution was then obtained by performing a projection operation in applying the gradient method. Numerical simulations for two typical clinical cases (for prostate and head-and-neck cancers, each for two patients) are given.

1. Introduction

Cancer is one of the most significant health problems in the world. One of the main treatment forms besides surgery and chemotherapy is radiation therapy. The concept of radiation therapy is that ionizing radiation is used to damage the DNA and interfere with cell division and cell growth.

Intensity-modulated radiation therapy (IMRT) is a state of the art technique for administering radiation to cancer patients. To achieve a terminal tumor dose, the surrounding critical organs are inevitably harmed. Thus we want to carefully control how much healthy tissue can be damaged in the process.

The primary delivery tool for IMRT is a linear accelerator that rotates on a gantry around the patient, emitting modulated beams of X - rays from a number of pre - fixed angles (see Figure 1. left). This modulation is accomplished by means of a device known as a multileaf collimator (MLC). Its computer - controlled leaves act as a filter, blocking or allowing radiation through in order to tailor the beam field to the shape of the tumor and minimize the exposure of the critical organs (see Figure 1. right). It is necessary to determine how the intensity of an X-ray beam should be at each point (x,y) on the MLC aperture surface for all gantry angles. These fluence maps are represented by nonnegative functions $I_a(x, y)$ for $a = 1, 2, ..., k$, where k is the number of gantry angles in use. $I_a(x, y)$ would be approximated with a set of discrete values $I_a(x_i, y_j)$ by discretizing the MLC aperture with nodes (x_i, y_j); therefore, we can show the unknown beamlet intensity $I_a(x_i, y_j)$, $a = 1, 2, \cdots, k$,

Received: August 2010; Revised: October 2010; Accepted: December 2010
Key words and phrases: IMRT, Singed distance, Triangular fuzzy number, Gradient method.




FIGURE 1. Left: Linear Accelerator, Right: MLC

for all beam angles by a single vector $x \in \mathbb{R}^n_+$, where n is the total number of the beamlets for all beam angles.

2. Dose-Volume Constraints and Dose Calculation

Radiation oncologists introduce dose-volume constraints (DVCs), which specify a given percentage of volume for each critical organ that can be sacrificed if necessary, while the tumor is given a prescribed amount of radiation. Each row of Table 1 represents a distinct dose-volume constraint for that structure. For example, the brain stem DVC specifies that no more than 10% of the voxels (defined below) in the brain stem may exceed a 40 Gray dose.

Structure	Dose	Volume
Target	70Gy	95%
Parotid Gland	21Gy	30%
Brain Stem	40Gy	10%
Spinal Cord	35Gy	10%

TABLE 1. Head and Neck- Dose- Volume Constrains.

The region of treatment is discretized into small three-dimensional rectangular elements, say voxels. If the absorbed dose values is defined by the voxels with a vector $d \in \mathbb{R}^m (m$ is the total number of voxels in the region of treatment), in a standard IMRT model we have $d_i = \sum_{j=1}^{n} a_{ij}\, x_j$ where a_{ij} gives the dose absorbed by the i-th voxel per unit intensity emission from the j-th beamlet. Matrix $A = [a_{ij}] \in \mathbb{R}_+^{(m_t+m_h)\times n}$ is called the influence matrix (m_t and m_h are the number of target and critical structure voxels, respectively); therefore, $d = Ax$. Since calculating A is quite expensive, currently dose computing is still considered as an important research area; here, we assume that A is provided by Computational Environment for Radiotherapy Research (CERR) software, (see [4]).

3. Current Practices and Researchs

The IMRT fluence map optimization problem has been extensively studied for a number of years. Several classes of optimization models have been proposed for fluence optimization.

Linear models have long been used in this problem. They offered very satisfactory theoretical results at the cost of a large number of constraints and variables (for example, see [10, 1, 12]).

The fluence map optimization problem also can be viewed as mixed integer programming (MIP)([11, 8]). The challenge of using MIP modeling for IMRT is that the resulting instances are very large-scale, and since general MIP is NP-hard, specialized algorithms designed to solve IMRT instances are required.

If an objective function is associated with each anatomical structure, then this problem can be naturally viewed as a multi-objective optimization problem. In multi-objective optimization, many different objective functions have been used for the fluence map problem in IMRT. In fact, many of these seemingly different approaches produce nearly the same Pareto optimal solutions (see [3, 6, 13]). Thus a model for fluence map planning has a multi-criteria nature of the problem. This is the most difficult challenge for determining optimality ([3]).

Also the least-squares models were the first practical models (for example, see [14]). The main advantage of these models is their speed and that they produce good results, but they have some natural limitations, such as non-convexity of the solution space.

But in all such literatures, the variables and parameters are considered as a crisp type; even in the real world, some of them are fuzzy, such as prescribed target dose vector parameter. Solving one of these is precisely our main focus of attention in this paper.

4. Description of Fuzzy Target Dose Vector

At first, we need the following fuzzy concepts:

Definition 4.1. For a fuzzy set $\tilde{A}$ defined on X and for any number $\alpha \in [0,1]$, the α-cut, $\tilde{A}^{\alpha}$ is defined as: $\tilde{A}^{\alpha} = \{x \mid \mu_{\tilde{A}}(x) \geq \alpha\}$ ([17]). That is, the α-cut of a fuzzy set $\tilde{A}$ is the crisp set $\tilde{A}^{\alpha}$ which contains all the elements of the universal set X whose membership grades in $\tilde{A}$ are greater than or equal to the specified value of α.

Definition 4.2. A fuzzy number is a fuzzy set $u : \mathbb{R} \to I = [0,1]$ which satisfies the following conditions:

1. u is upper semi-continuous,
2. $u(x) = 0$ outside some interval $[a,d]$,
3. There are real numbers a, b such that $a \leq b \leq c \leq d$ and

(a) $u(x)$ is monotonic increasing on $[a,b]$,

(b) $u(x)$ is monotonic decreasing on $[c,d]$,

(c) $u(x) = 1$, $b \leq x \leq c$.

The membership function u can be expressed as

$$u(x) = \begin{cases} u_L(x), & a \le x \le b; \\ 1, & b \le x \le c; \\ u_R(x), & c \le x \le d; \\ 0, & otherwise, \end{cases}$$

where $u_L : [a, b] \to [0, 1]$ and $u_R : [c, d] \to [0, 1]$ are left and right membership functions of fuzzy number u ([5]).

Definition 4.3. If the membership function of the fuzzy set $\tilde{A}$ on $\mathbb{R}$ is

$$\mu_{\tilde{A}}(x) = \begin{cases} (x-p)/(q-p), & p \le x \le q; \\ (r-x)/(r-q), & q \le x \le r; \\ 0, & otherwise, \end{cases} \quad (1)$$

where $p < q < r$, then $\tilde{A}$ is called a triangular fuzzy number. We denote $\tilde{A} \equiv (p, q, r)$ ([17]).

Definition 4.4. For each $a, b \in \mathbb{R}$, the signed distance of a from b is defined by $d^*(a, b) = a - b$.

If a be in the right or the left of b, the sign of d^* will be negative or positive respectively. Also, we have $d^*(a, b) = d^*(a, 0) - d^*(b, 0)$ ([15]).

Definition 4.5. For $p < q$ and $0 < \alpha \le 1$ if the membership function of the fuzzy set $[p_\alpha, q_\alpha]$ on $\mathbb{R}$ is

$$\mu_{[p_\alpha, q_\alpha]}(x) = \begin{cases} \alpha, & p \le x \le q; \\ 0, & otherwise, \end{cases} \quad (2)$$

then $[p_\alpha, q_\alpha]$ is called a level α fuzzy interval (see [2]).

As a fuzzy number, $\tilde{b_i}$ specifies the maximum and minimum dose absorbed for the i-th voxel of the target. For example, suppose that a prescription specifies the dose absorbed for the i-th voxel from 5Gy to 10Gy. These values have the most and the least degree of satisfaction respectively; for if the tumor absorbs less dose, the organs at risk will generally absorbs less dose too. Let the degree of satisfaction be normalized as a membership degree, by $b_{i_{min}} = 5$Gy with the membership degree 1 and $b_{i_{max}} = 10$Gy with the membership degree zero.

To be able to consider $\tilde{b_i} = (b_{i_{min}}, b_{i_{min}}, b_{i_{max}})$ as a triangular fuzzy number, it is enough to select p in Definition 3 as a number which is very very close to $b_{i_{min}}$, like $p = b_{i_{min}} - 10^{-5}$. Therefore, we consider $\tilde{b_i} = (b_{i_{min}} - 10^{-5}, b_{i_{min}}, b_{i_{max}})$ that its membership function is:

$$\mu_{\tilde{b_i}}(y) = \begin{cases} \frac{(y - b_{i_{min}} + 10^{-5})}{10^{-5}}, & b_{i_{min}} - 10^{-5} \le y \le b_{i_{min}}; \\ \frac{(b_{i_{max}} - y)}{(b_{i_{max}} - b_{i_{min}})}, & b_{i_{min}} \le y \le b_{i_{max}}; \\ 0, & otherwise; \end{cases}$$

the figure below represents this membership function.

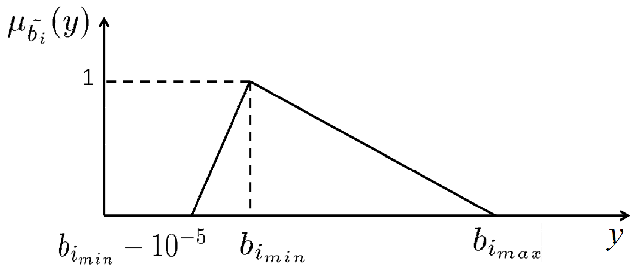


FIGURE 2. Membership Function of $\tilde{b_i}$

5. **Problem Formulation**

Let $D_v \subseteq \mathbb{R}_+^m$ be the set of dose vectors that satisfy all the dose-volume constraints for a given problem and let $\tilde{b_t} \in \mathbb{R}_+^{m_t}$ be a fuzzy prescribed target dose vector; also we assume that the rows of A are organized as $A^T = [A_t^T A_h^T]$, where A_t is the submatrix consisting of target voxel rows and likewise A_h is made of healthy tissue voxel rows. Then the prescription set H and the physical set K are defined as:

$$H = \left\{ \begin{bmatrix} \tilde{b_t} \\ u \end{bmatrix} : u \in D_v \right\} \subset \mathbb{R}_+^{m_t+m},$$
$$K = \left\{ \begin{bmatrix} A_t x \\ Ax + s \end{bmatrix} : x, s \geq 0 \right\} \subset \mathbb{R}_+^{m_t+m}.$$

Both H and K are closed sets in $\mathbb{R}_+^m$, and K is a convex cone; but H is non-convex, since the DVCs have a combinatorial nature ([9]). In fact, D_v is a non-convex union of convex boxes.

We would ideally like to find $x \in \mathbb{R}_+^n$ and $s \in \mathbb{R}_+^m$ that $A_t x = \tilde{b_t}$ and $Ax + s = u$. But the reality of the IMRT fluence problem is that there may be no physically-achievable dose that both satisfies the DVCs and meets the prescription. That is, generally speaking $dist(H, K) > 0$, or equivalently, $H \cap K = \phi$; thus, the goal is to obtain $d_H \in H$ and $d_K \in K$ that:

$$\begin{aligned} dist(H, K) &= \|d_H - d_K\| = min_{u \in D_v} dist \left(\begin{bmatrix} \tilde{b_t} \\ u \end{bmatrix} - K \right) \\ &= \min_{u \in D_v} \min_{x,s \geq 0} \left\| \begin{bmatrix} \tilde{b_t} \\ u \end{bmatrix} - \begin{bmatrix} A_t x \\ Ax + s \end{bmatrix} \right\|. \end{aligned} \tag{3}$$

The norm in the right-hand side of (3) can be replaced by

$$q(x, s, u) = \frac{1}{2}\|A_t x - \tilde{b_t}\|^2 + \frac{1}{2}\|Ax + s - u\|^2. \tag{4}$$

Thus, one can define our objective function as

$$f(u) = \min_{(x,s)\geq 0} q(x, s, u). \tag{5}$$

Now we re-pose the problem (3) with

$$\min_{u\in D_v} f(u). \tag{6}$$

It is not difficult to show that $f(u)$ decreases monotonically as u increases. Regardless of the fact that the parameter $\tilde{b_t}$ is fuzzy, there are many methods for solving the problem (6). To use the best one, we prefer first to defuzzyfy the problem.

6. **Defuzzying Process**

In the sense of [9], here, there exists an α-cut of $\tilde{b_i}$ for each $\alpha \in [0, 1]$; the left-hand point of an α-cut is $b_i^L\ (\ \alpha\ ) = p + (\ q - p)\ \alpha$ and the right-hand point of it is $b_i^U(\alpha) = r - (r - q)\alpha$ (see Figure 3). Therefore the α-cut of $\tilde{b_i}$ is $[b_i^L(\alpha), b_i^U(\alpha)]$. Corresponding to the crisp interval $[b_i^L(\alpha), b_i^U(\alpha)]$, we have the level α fuzzy interval $[b_i^L(\alpha)_\alpha, b_i^U(\alpha)_\alpha]$([2]). By (2) we have

$$\mu_{[b_i^L(\alpha)_\alpha, b_i^U(\alpha)_\alpha]}(x) = \begin{cases} \alpha, & b_i^L(\alpha) \leq x \leq b_i^U(\alpha); \\ 0, & otherwise. \end{cases}$$

As explained in section 2, the influence matrix A_t and the vector x are crisp; thus each component like $(A_t x)_i$ is also crisp. In the manner that has been explained in [2], we define the signed distance of the crisp interval $[b_i^L(\alpha), b_i^U(\alpha)]$ to the crisp number $(A_t x)_i$ as

$$\begin{aligned} d^*([b_i^L(\alpha), b_i^U(\alpha)], (A_t x)_i) &= \tfrac{1}{2}[d^*(b_i^L(\alpha), (A_t x)_i) + d^*(b_i^U(\alpha), (A_t x)_i)] \\ &= -(A_t x)_i + \tfrac{1}{2}[b_{i_{min}} + b_{i_{max}} + (b_{i_{min}} - b_{i_{max}})\alpha)]. \end{aligned}$$

Proposition 6.1. *The signed distance of the level α fuzzy interval $[b_i^L(\alpha)_\alpha, b_i^U(\alpha)_\alpha]$ from $(\tilde{A_t x})_i$ is*

$$d([b_i^L(\alpha)_\alpha, b_i^U(\alpha)_\alpha], (\tilde{A_t x})_i) = d^*([b_i^L(\alpha), b_i^U(\alpha)], (A_t x)_i).$$

Proof. It is obvious since the α - cut $[b_i^L(\alpha), b_i^U(\alpha)]$ and the level α fuzzy interval $[b_i^L(\alpha)_\alpha, b_i^U(\alpha)_\alpha]$ are one to one correspondence. □

Proposition 6.2. *The signed distance of $\tilde{b_i}$ from $(\tilde{A_t x})_i$ is*

$$\begin{aligned} d(\tilde{b_i}, (\tilde{A_t x})_i) &= \textstyle\int_0^1 d^*([b_i^L(\alpha), b_i^U(\alpha)], (A_t x)_i) d\alpha \\ &= \tfrac{1}{4}(3b_{i_{min}} + b_{i_{max}}) - (A_t x)_i. \end{aligned}$$

Proof. The function d in Proposition 1 is continuous with respect to α in [0, 1]; like in [2], we can use a definite integral to find its average value as distance. □

We remind that $(A_t x)_i$ is regarded as a fuzzy number $(\tilde{A_t x})_i$ by the usual one to one correspondence. Now we are able to represent the objective function of the problem by regarding the following proposition.

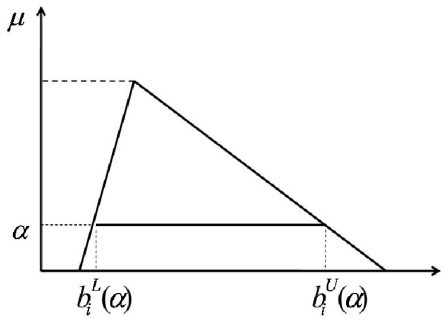


FIGURE 3. α- Cut of $\tilde{b_i}$

Proposition 6.3. *By introducing* $d(\tilde{b_t}, \tilde{A_t x}) = \sqrt{\sum_{i=1}^{m_t}(d(\tilde{b_i}, (\tilde{A_t x})_i))^2}$ *as a criterion for evaluating the proximity* $\tilde{b_t}$ *and* $\tilde{A_t x}$*, relation (5) in fuzzy environment is converted to:*

$$q(x,s,u) = \frac{1}{2}\|A_t x - \frac{3b_{min} + b_{max}}{4}\|^2 + \frac{1}{2}\|Ax + s - u\|^2.$$

Proof. We have

$$\begin{aligned} d(\tilde{b_t}, \tilde{A_t x}) &= \sqrt{\sum_{i=1}^{m_t}(d(\tilde{b_i}, (\tilde{A_t x})_i))^2} \\ &= \sqrt{\sum_{i=1}^{m_t}((3b_{i_{min}} + b_{i_{max}})/4) - (A_t x)_i)^2} \\ &= \|A_t x - ((3b_{min} + b_{max})/4)\|, \end{aligned}$$

where b_{min}=$(b_{1_{min}}, b_{2_{min}}, \ldots, b_{m_{t\,min}})$ and b_{max}=$(b_{1_{max}}, b_{2_{max}}, \ldots, b_{m_{t\,max}})$. Hence (4) is converted to the following one:

$$\begin{aligned} q(x,s,u) &= d(\tilde{b_t}, \tilde{A_t x}) + \tfrac{1}{2}\|Ax + s - u\|^2 \\ &= \tfrac{1}{2}\|A_t x - \tfrac{3b_{min}+b_{max}}{4}\|^2 + \tfrac{1}{2}\|Ax + s - u\|^2. \end{aligned}$$

□

Thus, by changing the fuzzy vector $\tilde{b_t}$ to a nonfuzzy vector b_t, the way of solving (6) in fuzziness state is the same as its nonfuzziness state, except that $\tilde{b_t}$ should be replaced by $\frac{3b_{min}+b_{max}}{4}$.

7. Solution Algorithm

For $u \in D_v$, it can be proved that f(u) is differentiable and

$$\begin{aligned} \nabla f(u) &= \nabla_u q(x(u), s(u), u) = -\max(Ax(u) - u, 0) \le 0, \\ s(u) &= \max(u - Ax(u), 0). \end{aligned}$$

The derivation of this formula is rather long (see [9]). The feasible set D_v is a non-convex set that consist of a large number of branches. Therefore, we can use the algorithm mentioned in [16] in which it seeks for a good local minimum of (6) in an efficient manner.

This algorithm uses a relaxation scheme based on the sensitivity of f and it is called Sensitivity-Driven Greedy (SDG) algorithm.

SDG Algorithm

-Input: Initial dose bound $u^0 \in D_v$.

-Output: Beamlet intensities $x(u^k)$.

for k = 0, 1, 2, . . .

(1) Solve $Q(u^k)$ for $x(u^k)$.

(2) Compute $\nabla f(u^k) = -\max(Ax(u^k) - u^k, 0)$.

(3) If stopping criteria are met, the output is $x(u^k)$ and stop.

(4) Set $u^{k+1} = Proj_{D_v^k}(u^k - \nabla f(u^k))$ where $D_v^k = \{u : u \geq u^k\} \cap D_v$.

endfor.

Our choice for u^0 is the prescribed dose bounds at the lowest level DVCs. Note that in step 4 the inside vector of the projection operator is

$$u^k - \nabla f(u^k) \equiv \max(u^k, Ax(u^k)) \geq u^k.$$

Hence, a dose bound u_i^k is replaced by the calculated dose value $[Ax(u^k)]_i$ whenever the latter is greater. The resulting larger vector is then projected onto the set D_v^k to obtain the next dose bound u^{k+1}. The following theorem shows that this algorithm is convergence (see [16]).

Theorem 7.1. *If A is a full column rank matrix, then the Sensitivity-Driven Greedy Algorithm, without stopping, generates an infinite sequence $\{u_k\}$ that converges to a local minimum of f in D_v.*

The bulk of the computation in the SDG algorithm is to solve the subproblem $Q(u^k)$ in Step 1 at each iteration which is a convex quadratic program, known as a non-negative least-squares (NNLS) problem. Considering their relative large sizes in IMRT applications, a fast algorithm for solving these NNLS problems is of primary importance. On the other hand, due to errors in leaf-sequencing, measurement, imaging, dose calculation, patient motion and etc., high accuracy solutions are not necessary. Like [9], in our implementation, we use an interior-point gradient (IPG) algorithm that was originally designed to strike a balance between reasonable accuracy and efficiency in this application. The IPG algorithm is presented in the appendix of this paper.

8. **Simulations and Results**

In our experiments, we used the quadrant infinite beam (QIB) dose calculation engine within CERR to generate an influence matrix for each test case using five equally-spaced beams. Our numerical experiments have been conducted on head-and-neck and prostate cases.

In IMRT, the DVC compliance is visualized by cumulative dose-volume histograms (DVHs), where the x-axis presents the dose values and the y-axis presents the accumulated volume percentage. In the DVH, each planning structure has a corresponding curve. The ideal curve for a target structure is a step function dropping from 100 to zero at the prescribed dose value. For a healthy structure, the

lower curve is the better. On the other hand, a dose distribution satisfies the DVC if the curve is below or goes through the corresponding point.

The DVCs and DVHs for two typical clinical head-neck and prostate cases (each case for two patients) are given in Tables 2-5 and in Figures 4-7, respectively; where GTV stands for gross target volume. For showing target dose in the DVHs, as calculated in our method the crisp number $b_t = \frac{3b_{min}+b_{max}}{4}$ is used instead of the fuzzy number $\tilde{b_t}$.

As Figures 4-7 show, for both patients A and B, the DVH curves of brain stem, parotid gland, bladder and rectum satisfy DVCs and the DVH curves of GTV as well as target, decrease near the DVC point with a very high tangent. Also 95% of GTV and target volume are completely located between the lower and upper bounds of $\tilde{b_t}$, where they are presented by dash lines parallel to the y-axis. Moreover, as seen in the figures, the curves are nearer to the lower bound compared to the upper bound; this indicates that besides satisfying the target dose coverage, the absorbed dose by the healthy organs are lessen. These facts show that the obtained treatment plan by our method, is suitable clinically.

Structure	Dose	Volume
Target	$60Gy \leq \tilde{b_t} \leq 100Gy$	95%
Parotid Gland	21Gy	30%
Brain Stem	40Gy	10%

Table 2. Head and Neck A- Dose- Volume Constrains

Structure	Dose	Volume
Target	$60Gy \leq \tilde{b_t} \leq 100Gy$	95%
Parotid Gland	15Gy	40%
Brain Stem	13Gy	30%

Table 3. Head and Neck B- Dose- Volume Constrains

Structure	Dose	Volume
GTV	$71Gy \leq \tilde{b_t} \leq 99Gy$	95%
Bladder	47Gy	53%
Rectum	75Gy	30%

Table 4. Prostate A- Dose- Volume Constrains

Structure	Dose	Volume
GTV	$70Gy \leq \tilde{b_t} \leq 98Gy$	95%
Bladder	47Gy	34%
Rectum	47Gy	58%

Table 5. Prostate B- Dose- Volume Constrains

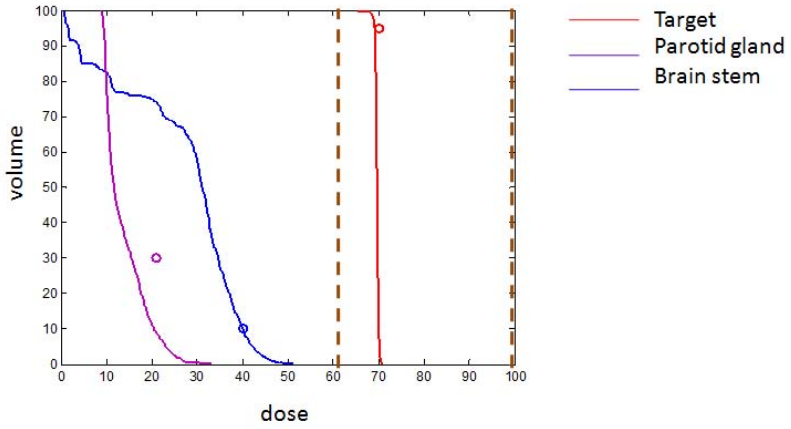


FIGURE 4. Head and Neck A- DVH of $\tilde{b}_i$

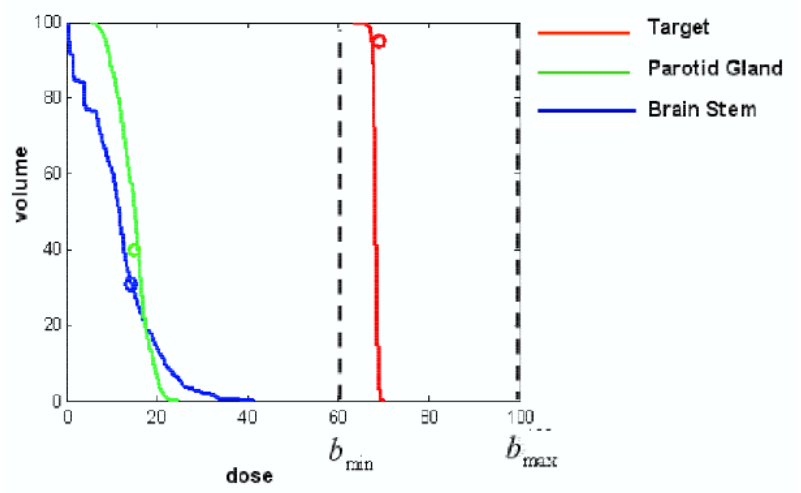


FIGURE 5. Head and Neck B- DVH of $\tilde{b}_i$

9. **Conclusion**

Even in reality, some parameters in IMRT optimization model are fuzzy, but there was no any known method for solving this kind of problems. For the case that the target dose vector is fuzzy, here, we presented an effective and applicable optimization method, regardless the nonconvexity of the solution space. This method is converged to the optimal solution with acceptable speed. Moreover, the numerical results have the efficient adaptation to the clinical experiments and analytically satisfy physicians. The results obtained in this study indicate that the described optimization method can be a useful tool in IMRT treatment planning.

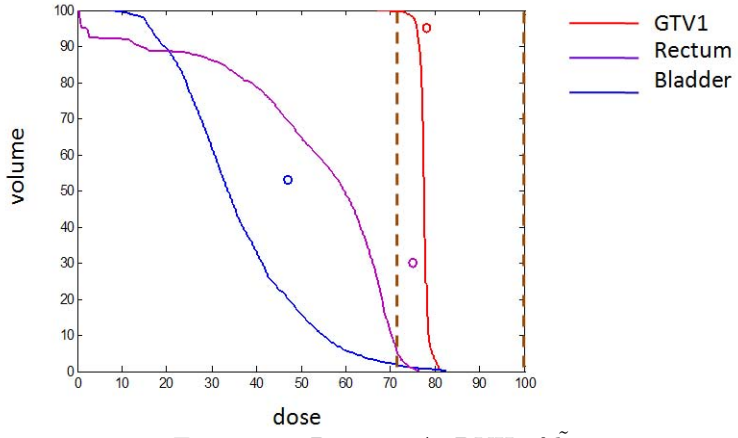


FIGURE 6. Prostate A- DVH of $\tilde{b}_i$

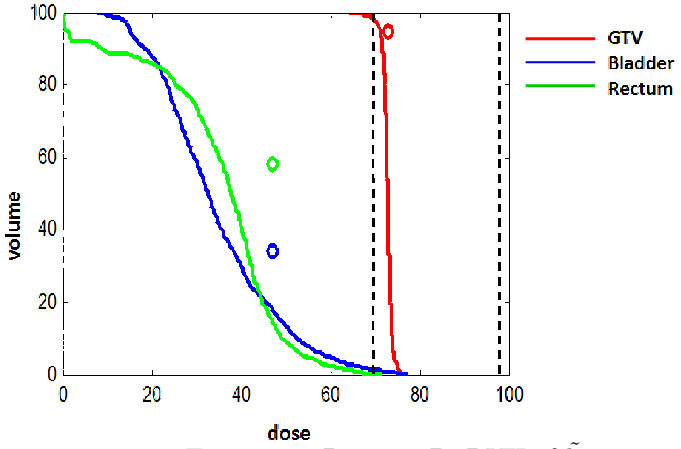


FIGURE 7. Prostate B- DVH of $\tilde{b}_i$

Appendix. Interior-Point Gradient Algorithm for solving NNLS Problem:

-Inputs: $A, b, \tau \in (0,1), x^0 > 0$
-Output: Approximate solution x^k
for k = 0, 1, 2, . . .

(1) Compute $\nabla q^k = A^T Ax^k - A^T b$, and set $p^k = -d^k \circ \nabla q^k$, where $d_i^k = \frac{x_i^k}{(A^T Ax^k)_i}$.
(2) Check stopping condition.

(3) Choose $\tau_k \in [\tau, 1)$ and set $\alpha_k = min(\tau_k \hat{\alpha_k}, \alpha_k^*)$, where $\hat{\alpha_k} = max \{ \alpha : x^k + \alpha p^k \geq 0 \}$ and $\alpha_k^* = -\frac{(p^k)^T \nabla q^k}{(p^k)^T A^T A p^k}$.

(4) Set $x^{k+1} = x^k + \alpha_k p^k$.

endfor.

Acknowledgements. Some of the authors are supported in parts by Fuzzy Systems and Applications Center of Excellence, Shahid Bahonar University of Kerman, I. R. of Iran.

References

[1] G. Bahr, J. Kereiakes, H. Horwitz, R. Finnery, J. Calvin and K. Goode, *The method of linear programming applied to radiation treatment planning*, Radiology, **91** (1968), 686-693.

[2] J. Chiang, *Fuzzy linear programming based on statistical confidence interval and interval-valued fuzzy set*, European Journal of Operational Research, **129** (2001), 65-86.

[3] C. Cotrutz, M. Lahanas, C. Kappas and D. Baltas, *A multiobjective gradient based dose optimization algorithm for external beam conformal radiotherapy*, Physics in Medicine and Biology, **46** (2001), 2161-2175.

[4] J. Deasy, A. Blanco and V. Clark, *Cerr: a computational environment for radiotherapy research*, Medical Physics, **30** (2003), 979-985.

[5] D. Dubois and H. Prade, *Fuzzy sets and systems: theory and application*, Academic Press, New York, 1980.

[6] H. W. Hamacher and K. H. Kufer, *Inverse radiation therapy planninng - a multiple objective optimization approach*, Discrete Applied Mathematics, **118** (2002), 145-161.

[7] C. L. Lawson and R. J. Hanson, *Solving least squares problems*, SIAM, (1995), 160-165.

[8] E. Lee, T. Fox and I. Crocker, *Integer programming applied to intensity modulated radiation therapy treatment planning*, Annals of Operations Research, **119** (2003), 165-181.

[9] M. S. Merritt, *A sensitivity-driven greedy approach to fluence map optimization in intensity-modulated radiation therapy*, Ph. D. thesis, Department of Computational and Applied Mathematics, Rice University, April 2006.

[10] S. Morrill, R. Lane, J. Wong and I. Rosen, *Dose-volume considerations with linear programming optimization*, Medical Physics, **18** (1991), 1201-1210.

[11] F. Preciado-Walters, M. Langer, R. Rardin and V. Thai, *A coupled column generation, mixed-integer approach to optimal planning of intensity modulated therapy for cancer*, Mathematical Programming, **101** (2004), 319-338.

[12] H. E. Romeijn, R. K. Ahuja, J. F. Dempsey, A. Kumar and G. J. Li, *Novel linear programming approach to fluence map optimization for intensity modulated radiation therapy treatment planning*, Physics in Medicine and Biology, **48** (2003), 3521-3542.

[13] H. E. Romeijn, J. F. Dempsey and J. G. Li, *A unifying framework for multi criteria fluence map optimization models*, Physics in Medicine and Biology, **49** (2004), 1991-2013.

[14] S. V. Spirou and C. Chui, *A gradient inverse planning algorithm with dose-volume constraints*, Medical Physics, **25** (1998), 321-333.

[15] J. Yao and K. Wu, *Ranking fuzzy numbers based on decomposition principle and signed distance*, Fuzzy Sets and Systems, **116** (2000), 275-288.

[16] Y. Zhang and M. Merrit, *Dose-volume-based IMRT fluence optimization: a fast leastsquares approach with differentiability*, Linear Algebra and its Applications, **428** (2008), 1365-1387.

[17] H. J. Zimmermann, *Fuzzy set theory and its applications*, second ed., Kluwer Academic Publishers, Boston, 1991.

Alireza Fakharzadeh Jahromi*, Shiraz University of Technology, Shiraz, Fars, Iran
E-mail address: a_fakharzadeh@sutech.ac.ir

Omolbanin Bozorg, Shiraz University of Technology, Shiraz, Fars, Iran
E-mail address: o.bozorg@gmail.com

Hamidreza Maleki, Shiraz University of Technology, Shiraz, Fars, Iran
E-mail address: maleki@sutech.ac.ir

Mohamad Amin Mosleh-Shirazi, Shiraz University of Medical Sciences, Shiraz, Fars, Iran
E-mail address: mosleh_amin@hotmail.com

*Corresponding author